Metabolic Engineering 80 (2023) 241–253

Contents lists available at ScienceDirect

Metabolic Engineering

journal homepage: www.elsevier.com/locate/meteng

Establishing a versatile toolkit of flux enhanced strains and cell extracts for pathway prototyping

Xiunan Yi [a,b,1], Blake J. Rasor [c,d,e,1], Nathalie Boadi [c,d,e], Katherine Louie [f], Trent R. Northen [f], Ashty S. Karim [c,d,e], Michael C. Jewett [c,d,e,g,**], Hal S. Alper [a,b,*]

[a] Institute for Cellular and Molecular Biology, The University of Texas at Austin, Austin, TX, 78712, USA
[b] McKetta Department of Chemical Engineering, The University of Texas at Austin, Austin, TX, 78712, USA
[c] Department of Chemical and Biological Engineering, Northwestern University, Evanston, IL, 60208, USA
[d] Chemistry of Life Processes Institute, Northwestern University, Evanston, IL, 60208, USA
[e] Center for Synthetic Biology, Northwestern University, Evanston, IL, 60208, USA
[f] DOE Joint Genome Institute, Lawrence Berkeley National Laboratory, Berkeley, CA, 94720, USA
[g] Department of Bioengineering, Stanford University, Stanford, CA, 94305, USA

ARTICLE INFO

Keywords:
Cell-free
Pathway prototyping
Biomanufacturing

ABSTRACT

Building and optimizing biosynthetic pathways in engineered cells holds promise to address societal needs in energy, materials, and medicine, but it is often time-consuming. Cell-free synthetic biology has emerged as a powerful tool to accelerate design-build-test-learn cycles for pathway engineering with increased tolerance to toxic compounds. However, most cell-free pathway prototyping to date has been performed in extracts from wildtype cells which often do not have sufficient flux towards the pathways of interest, which can be enhanced by engineering. Here, to address this gap, we create a set of engineered *Escherichia coli* and *Saccharomyces cerevisiae* strains rewired via CRISPR-dCas9 to achieve high-flux toward key metabolic precursors; namely, acetyl-CoA, shikimate, triose-phosphate, oxaloacetate, α-ketoglutarate, and glucose-6-phosphate. Cell-free extracts generated from these strains are used for targeted enzyme screening *in vitro*. As model systems, we assess *in vivo* and *in vitro* production of triacetic acid lactone from acetyl-CoA and muconic acid from the shikimate pathway. The need for these platforms is exemplified by the fact that muconic acid cannot be detected in wildtype extracts provided with the same biosynthetic enzymes. We also perform metabolomic comparison to understand biochemical differences between the cellular and cell-free muconic acid synthesis systems (*E. coli* and *S. cerevisiae* cells and cell extracts with and without metabolic rewiring). While any given pathway has different interfaces with metabolism, we anticipate that this set of pre-optimized, flux enhanced cell extracts will enable prototyping efforts for new biosynthetic pathways and the discovery of biochemical functions of enzymes.

1. Introduction

Sustainable biomanufacturing practices often employ engineered cells to produce both specialty and commodity chemicals (Ekas et al. 2019; Liu and Nielsen 2019). To engineer cells, multiple approaches are used. These approaches include designing and tuning DNA cassettes to balance heterologous enzyme expression levels, selecting the best enzymes for the desired chemistries, and modifying native metabolic pathways to channel flux towards the desired product, among others. Workflows aimed at these goals are often slowed by time-consuming design-build-test-learn cycles and a constant battle between the evolutionary drive of cells to grow and the engineered capacity to overproduce a compound through rewiring (Karim and Jewett 2016).

While cell-based, high-throughput screening approaches can aid in efforts to engineer cells (d'Oelsnitz et al., 2022; Li et al., 2020; Liu et al., 2018; Rogers et al. 2016; Tenhaef et al., 2021; Wehrs et al., 2020), the use of cell-free pathway prototyping strategies has recently emerged as an approach to speed up metabolic engineering design-build-test-learn cycles (Bergquist et al. 2020; Bowie et al., 2020; Dudley et al., 2020; Karim and Jewett 2018; Liew et al., 2022; Moore et al., 2023; O'kane

* Corresponding author. Institute for Cellular and Molecular Biology, The University of Texas at Austin, Austin, TX, 78712, USA.
** Corresponding author. Department of Bioengineering, Stanford University, Stanford, CA, 94305, USA.
E-mail addresses: mjewett@stanford.edu (M.C. Jewett), halper@che.utexas.edu (H.S. Alper).
[1] These authors contributed equally.

https://doi.org/10.1016/j.ymben.2023.10.008
Received 9 August 2023; Received in revised form 7 October 2023; Accepted 23 October 2023
Available online 26 October 2023

et al., 2019; Rasor et al., 2022; Vögeli et al., 2022). Cell-free approaches enable rapid screening of hundreds of pathway combinations in a matter of weeks, rather than months or years (Bogart et al., 2021; Karim and Jewett 2018; Lim and DongKim, 2019; Rasor et al., 2022). Cell extracts derived from *E. coli* are even able to predict pathway performance in non-model organisms like *Clostridium autoethanogenum* to down-select promising enzyme combinations for *in vivo* testing (Karim et al., 2020; Liew et al., 2022; Vögeli et al., 2022).

To date, nearly all examples of cell-free prototyping utilize wildtype cell extracts (Dudley et al., 2020; Karim et al., 2020; Kelwick et al., 2018; Liew et al., 2022). While this approach can help in the functional characterization of heterologous pathways, the net carbon flux towards certain pathway precursors in these wild-type cell-free reactions can be inherently limited. However, this is not the case for *in vivo* systems wherein extensive strain engineering is typically conducted to both detect and improve metabolite production. Moreover, numerous *in vivo* studies have shown that the variations of native metabolism alone from distinct host organisms can lead to significant differences in the production of biosynthetic pathways (Deaner et al. 2018; Gambacorta et al., 2020; Papagianni 2012; Yi and Alper 2022).

Strain rewiring is particularly useful for energy-intensive or highly regulated pathways where the carbon flux is significantly altered in production strains to compensate for significant metabolic burden (Wu et al., 2016). For example, biochemical products derived from the shikimate pathway (including muconic acid (Curran et al., 2013), alkaloids (Khatri et al., 2020; Milne et al., 2020; Srinivasan and Smolke 2020), and dopamine (Fordjour et al., 2019; Galanie et al., 2015)), require large investments of carbon and energy bound by strict metabolic regulation (Averesch and Krömer 2018).

Rerouting carbon flux through enzyme overexpression and/or transcriptional rewiring has become commonplace in biochemical production, but testing enzyme variants in engineered cell extracts is not. In this work, we posit that the extract derived from a rewired background cell will be reflective of the underlying proteome changes and thus potentiate the same metabolic flux patterning. Specifically, we sought to expand the product space and throughput of cell-free biosynthesis using extracts derived from both bacterial and eukaryotic systems. The goal was to generate platform strains with enhanced carbon flux toward common nodes of metabolism and then use cell extracts derived from these platform strains to rapidly screen biosynthetic pathways consisting of purified enzymes for high-throughput prototyping and optimization (Fig. 1). To accomplish this, we first engineered both *Escherichia coli* and *Saccharomyces cerevisiae* for increased flux toward 5 different metabolic branch points. Second, cell extracts were prepared from these rewired strains to enable accelerated pathway prototyping. Third, the approach was explored for a single-step heterologous pathway (toward triacetic acid lactone) and a multi-step heterologous pathway (toward muconic acid). The former highlighted additional points of inquiry for metabolic flux in cell-free systems relative to living cells, while the latter demonstrated that metabolic rewiring was essential for sufficient flux to detect the end product and that high-performing enzymes can be rapidly identified for cellular design. Overall, this work establishes a new concept for biochemical production, enzyme screening, and functional genomics across diverse branches of metabolism through a suite of flux-enhanced strains of bacteria and yeast. While any given pathway has different interfaces with metabolism, it is anticipated that this suite of strains along with corresponding cell extracts are collectively capable of improving the metabolic performance of cellular production strains.

2. Materials and methods

2.1. Strains and media

The *S. cerevisiae* strain BY4741 was used in this study. Complete

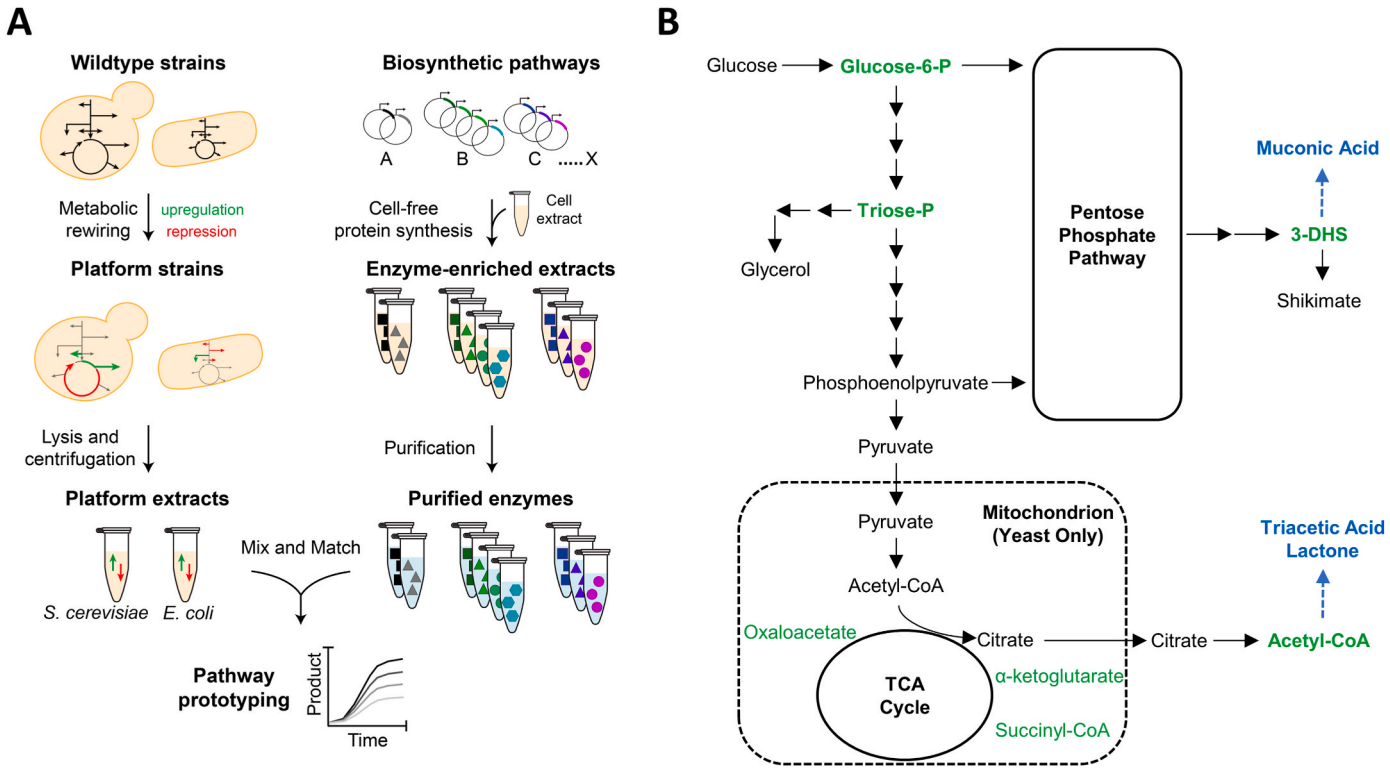

Fig. 1. Workflow for pathway prototyping toolkit generation and implementation. A) Cells are engineered for increased flux toward desired metabolic nodes, then these platform strains are converted into cell extracts to perform biosynthesis in the absence of growth or viability constraints. Panels of enzyme variants were synthesized by cell-free gene expression (CFE), purified, and then mixed with the platform extracts for metabolite synthesis from glucose. **B)** Metabolic map highlighting versatile branch points for increased flux (red) and potential products (blue) for engineered strains.

synthetic media containing 6.7 g/L of yeast nitrogen base with ammonium sulfate (AMRESCO), a complete supplement mixture (CSM) with appropriate dropout(s) (Sunrise Science Products and MP Biomedicals), and glucose (MP Biomedicals) were used to for BY4741 cultures. CSM with appropriate dropout(s) was added to 1 × concentration to enforce plasmid retention according to product specifications. For seed cultures, 20 g/L of glucose was added. For *in vivo* fermentations, 50 g/L of glucose was added.

The *E. coli* strain MG1655 was used in this study. LB media containing 25 g/L of premixed LB powder (Teknova) and corresponding antibiotics (100 mg/L of ampicillin, 50 mg/L of spectinomycin, and/or 30 mg/L of chloramphenicol) were used for the selections (additional 18 g/L of agar was added to make LB plates) and seed cultures. Rich M9 media containing M9 salt (Sigma), 2 mM $MgCl_2$, 0.1 mM $CaCl_2$, 1 g/L of casamino acid (Fisher BioReagents), 0.1 g/L of leucine (Sigma), 0.3 g/L of thiamine hydroxy acid (Fisher BioReagents), 20 g/L of glucose and corresponding antibiotics were used for *in vivo* fermentations.

The *E. coli* cloning strain NEB 10β was used in this study to construct plasmids. LB media and LB plates with corresponding antibiotics were used for transformant selection and cultures for plasmid miniprep.

2.2. Cloning method and transformations

All cloning reagents including Q5 Hot Start Polymerase, T4 Ligase, Gibson Master Mix, and various restriction enzymes were from New England Biolabs (NEB). PCR amplifications were conducted using BIO-RAD Thermal Cycler T100 or S1000 following the manufacturer's standard protocol. The primers were synthesized from Integrated DNA Technologies (IDT). The primers' annealing temperatures were calculated using NEB Tm Calculator.

To construct the yeast platform strains, the CRISPR rewiring systems were built as following. The control plasmid p415-dCas9VPR was from a previous study (Deaner et al., 2018). The rewiring plasmids were constructed with a 3-step cloning process. First, generation of tRNA-sgRNA fragments was achieved via primer annealing and ligation to pre-designed tRNA entry plasmids (Deaner et al., 2018). Second, tRNA-sgRNA fragments were PCR amplified and the restriction sites BsmBI was added. The tRNA-sgRNA fragments were linked into sgRNA cassettes on a pYTK001 backbone (Lee et al., 2015) using GoldenGate cloning with BsmBI-v2 and T4 Ligase. Last, p415-dCas9VPR was digested with HpaI and the sequenced sgRNA cassettes were PCR amplified and homologs for Gibson Assembly were added via primers. Plasmid backbone and sgRNA cassette inserts were ligated at 50 °C for 1 h using Gibson Assembly Master Mix.

To validate the yeast platform strains, the pathway plasmids were built as follows. The pathway genes were PCR amplified from the Joint Genome Institute (JGI) gene library (Supplementary Table S1). Corresponding restriction sites or homologs for Gibson Assembly were added via primers. Mumberg plasmids p416 with various expression promoters were digested with corresponding restriction enzymes overnight at 37 °C. Plasmid backbone and pathway inserts were ligated overnight at 16 °C using T4 Ligase or at 50 °C for 1 h using Gibson Assembly Master Mix. For single gene pathways, TDH3 promoter was used to build the expression cassette. For multi gene pathways, TPI1, PGK1, FBA1, and CYC1 promoters were used to build the expression cassette (ranking from high priority to low priority). The expression cassettes were then PCR amplified with new homologs for Gibson Assembly and assembled into one p416 plasmid. To build a yeast test strain with dual fluorescent markers. yECitrine (YFP) and mKate2 (RFP) were cloned into TPI1 and PGK1 expression cassettes as above and the whole cassettes were integrated into the BY4741 genome (TPI1-yECitrine::*trp1* and PGK1-mKate2::*leu2*). To achieve the integration, 500 bp homology arms were added to the linear fragment of expression cassettes by PCR amplification.

To construct the *E. coli* platform strains, the CRISPR rewiring systems were built as follows. The control plasmid pACYC-dCas9 was built by inserting the dCas9 expression cassettes into the plasmid. The dCas9 was expressed using the promoter and ribosome binding site from native *E. coli* gene *yccFS*. The rewiring plasmids were constructed with a 3-step cloning process. First, generation of sgRNA fragments was achieved via primer annealing and ligation to pre-designed sgRNA entry plasmids. This plasmid was built in this study and the guide RNAs after primer annealing were inserted between synthetic promoter J23109 and scaffold RNA to generate individual sgRNA expression cassettes. Second, individual sgRNA fragments were PCR amplified and the restriction sites BsmBI was added. The sgRNA fragments were linked into sgRNA cassettes on a pYTK001 backbone (Lee et al., 2015) using GoldenGate cloning with BsmBI-v2 and T4 Ligase. Last, the sgRNA cassettes were assembled into pACYC-dCas9 with Gibson Assembly after the homologs were added via PCR amplification.

E. coli rewiring also required overexpression of the native genes. These genes were PCR amplified and synthetic ribosome binding sites B31 or B32 as well as the restriction sites BsmBI were added. These genes were assembled into an expression plasmid with IPTG inducible promoter pTac into a polycistronic expression system (Sørensen and Kim-Mortensen, 2005). To validate the *E. coli* platform strains, the pathway plasmids were built as follows. The pathway genes were PCR amplified from the JGI gene library (Supplementary Table S1). Synthetic ribosome binding sites B31 or B32 as well as the restriction sites BsmBI were added via primers. These genes were assembled into an expression plasmid pCDF with the promoter from native *E. coli* gene *lpp* into a polycistronic expression system. To build the *E. coli* test strain, sfGFP gene was cloned as above into pCDF-lpp expression plasmid and introduced into *E. coli* MG1655. The plasmids were sequentially transformed into *S. cerevisiae* BY4741 or *E. coli* MG1655 and maintained on selective plates to build and validate the platform strains. The transformation protocols were as below.

For *E. coli* transformations, 50 μL of electrocompetent *E. coli* 10β was mixed with 50 ng of ligated DNA, Gibson Assembly reaction, or GoldenGate reaction and electroporated (2 mm Electroporation Cuvettes, Bioexpress) with a BioRad Genepulser Xcell at 2.5 kV. Transformants were shortly recovered in 1 mL of LB media, plated on LB agar supplemented with corresponding concentration of antibiotics, and incubated overnight at 37 °C. Single clones were amplified in 4 mL LB media supplemented with antibiotics and incubated overnight at 37 °C. Plasmids were isolated (GeneJET Plasmid Miniprep Kit, Thermo Scientific) and confirmed by Sanger or whole-plasmid sequencing. Then the constructed plasmids were transformed into electrocompetent *E. coli* MG1655 with 1 ng of DNA. For yeast transformations, 50 μL of chemically competent *S. cerevisiae* cells was transformed with 300 ng of pathway plasmids using Frozen-EZ Yeast Transformation II Kit (Zymo Research) according to the manufacturer's instructions. Transformations were plated on CSM with the appropriate dropout(s) and incubated for 2 days at 30 °C.

2.3. Metabolic rewiring via CRISPR

Overall, dCas9-VPR is expressed as a dual-mode regulator under the control of TDH3 promoter on a p415 Mumberg plasmid. On the same plasmid, a single guide RNA (sgRNA) cassette including sgRNAs targeting genomic DNAs is expressed under the control of TEF1 promoter. gRNA sequences are provided in Supplementary Table S2. The design of tRNA-sgRNA bricks is applied in the sgRNA cassette (Supplementary Table S3). After being expressed, tRNAs will be cut by Rnase P and Z to release the processed sgRNAs. For the control strains, a p415 plasmid containing the same TDH3-dCas9-VPR but no sgRNA cassette is used.

2.4. Cell extract preparation

Extracts were prepared from 1 L cell cultures according to established protocols with slight variations (Hodgman and Jewett 2013; Jewett and Swartz 2004; Karim and Jewett 2018; Kwon and Jewett

2015; Rasor et al., 2021, 2022). Materials were kept on ice at all times, and centrifuges were held at 4 °C. *E. coli* MG1655 cells with portable metabolic rewiring plasmids were grown in 2xYTPG media (16 g/L tryptone, 10 g/L yeast extract, 5 g/L NaCl, 7 g/L K_2HPO_4, 3 g/L KH_2PO_4, and 18 g/L glucose adjusted to pH 7.2 with KOH) from OD_{600} 0.08 to 0.1 before induction with 200 μM IPTG, after which they were grown for ~4 h. The cells were pelleted by centrifugation at 5,000×*g* for 10 min and washed in an acetate-based buffer (10 mM Tris base (from 1 M stock adjusted to pH 8.2 with acetic acid), 14 mM magnesium acetate, and 60 mM potassium acetate) three times, centrifuging for 2 min at 10,000×*g* between washes. The washed cell pellets were flash-frozen in liquid nitrogen, resuspended in 1 mL acetate buffer per gram of biomass, and lysed with an Avestin EmulsiFlex-B15 homogenizer at ~25,000 psi. The lysates were centrifuged for 10 min at 12,000×*g*, and the resulting supernatant was flash-frozen in aliquots as the final cell extract. BL21-Star (DE3) extract for cell-free gene expression was prepared in a similar manner but with induction at OD 0.6 and harvest at OD 3 for more active transcription/translation machinery.

S. cerevisiae extracts were prepared as previously described with minor modifications (Hodgman and Jewett 2013). Cells were grown in synthetic complete media (1.71 g/L yeast nitrogen base (Sunrise Science Products), 5 g/L ammonium sulfate, 20 g/L glucose, and a complete supplement mixture with the appropriate amino acid dropouts for auxotrophic selection) to OD_{600} 6–8, pelleted by centrifugation at 4, 000×*g* for 10 min, and washed in a glutamate-based buffer (30 mM HEPES adjusted to pH 7.4 with potassium hydroxide, 100 mM potassium glutamate, and 2 mM magnesium glutamate) three times, centrifuging for 5 min at 4,000×*g* between washes. The washed cell pellets were flash-frozen in liquid nitrogen, resuspended in 1 mL glutamate buffer per gram of biomass, and lysed with an Avestin EmulsiFlex-B15 homogenizer at ~30,000 psi. The lysates were centrifuged for 5 min at 20, 000×*g*, and the resulting supernatant was flash-frozen in aliquots as the final cell extract. This protocol was modified to omit the dialysis step for preparing *S. cerevisiae* extracts to better preserve cofactors and metabolic precursors synthesized during growth (Supplementary Fig. S5).

2.5. Cell-free biosynthesis reactions

Cell-free protein synthesis was performed by combining cell extract from *E. coli* BL21-Star(DE3) with linear expression templates and the PANOx-SP reaction formulation according to established protocols (Jewett et al., 2008; Jewett and Swartz 2004; Rasor et al., 2022). Enzymes were purified from cell-free protein synthesis reactions using Strep-Tactin beads or resin (IBA Lifesciences) and subsequently dialyzed into a buffer more similar to cell-free reaction compositions (100 mM BisTris, 100 mM potassium glutamate, 10 mM sodium phosphate). The enzymes were combined with cell extracts in 10 μL reactions for metabolite synthesis in 1.5-mL microcentrifuge tubes. TAL synthesis reactions contained 120 mM glucose, 10 mg/mL cell extract, 1 μM enzyme, 1 mM each of ATP, coenzyme A, and NAD, glutamate salts (8 mM magnesium glutamate, 10 mM ammonium glutamate, 134 mM potassium glutamate), and 100 mM BisTris buffer. Muconic acid synthesis reactions contained 120 mM glucose, 10 mg/mL cell extract, 0.5 μM of each enzyme, 3 mM ATP and NAD, 1 mM coenzyme A, glutamate salts (as above), and 100 mM BisTris buffer. All reactions were incubated at 30 °C for up to 20 h prior to precipitation with trichloroacetic acid and centrifugation for metabolite analysis. Samples were run on an Agilent 1260 HPLC with an 80:20 mixture of 0.1% formic acid in water and acetonitrile at 0.3 mL/min on a Luna® 3 μm C18(2) 100 Å LC Column.

2.6. Growth and fermentation conditions

For flow cytometry assays, the *S. cerevisiae* cultures were inoculated at OD (600 nm) = 0.01 into 3.5 mL of complete synthetic media (20 g/L of glucose). After 16 h, the fluorescence was measured using flow cytometry. Similarly, *E. coli* cultures were inoculated at OD (600 nm) = 0.01 into 3.5 mL of Rich M9 with corresponding antibiotics. After 8 h, the fluorescence was measured using flow cytometry.

All fermentation was conducted in 14 mL culture tubes. For *S. cerevisiae* fermentations, 3.5 mL of complete synthetic media (50 g/L of glucose) was inoculated at OD (600 nm) = 0.01 for each strain. For *E. coli* fermentations, 3.5 mL of Rich M9 with corresponding antibiotics was inoculated at OD (600 nm) = 0.01 for each strain. All cultures were incubated at 30 °C with 225 RPM shaking for 72 h. The fermentation was conducted with three biological replicates.

2.7. Quantification of in vivo products

Samples (1 mL) were taken after fermentation and centrifuged at 16,000 g. The supernatant was filtered with a 0.2 μm sterile syringe filter (VWR International) prior to high-performance liquid chromatography (HPLC) analysis.

For glucose and glycerol analysis, samples were separated using an HPLC Ultimate 3000 (Dionex) equipped with an Aminex HPX-87H ion exclusion column (BioRad) and analyzed using the Chromeleon 7.2 Chromatography Data System (Dionex). A 10 μL injection volume was used in an isocratic mobile phase of 5 mM H_2SO_4 (pH = 2) at a flow rate of 0.6 mL/min. The column temperature was 60 °C and a refractive index detector (RID) was used at a temperature of 25 °C. Standard curves were prepared using D-(+)-Glucose Anhydrous (MP Biomedicals) and glycerol (Sigma-Aldrich).

For 3-dehydroshikimate (3-DHS) analysis, a Zorbax SB-Aq column (Agilent Technologies) was used with the same HPLC system. 0.1% trifluoroacetic acid (TFA) in water or acetonitrile used as the mobile phase. The mobile phase started with 5% organic at 0.25 mL/min for 10 min, and was ramped from 5% organic to 100% organic, with a flowrate being ramped to 1 mL/min over 4 min. The mobile phase ratio and flowrate then gradually went back to the initial condition over 10 min. The column temperature was 30 °C and the UV at 215 nm was used for detection. A standard curve was prepared using 3-DHS standard (Sigma-Aldrich).

For muconic acid analysis, the same Zorbax SB-Aq column (Agilent Technologies) was used with the same HPLC system. 0.1% TFA in water or acetonitrile used as the mobile phase. The mobile phase was 16% organic (0.1 % TFA in acetonitrile) and 84% inorganic (0.1 % TFA in water) with a flowrate being 1 mL/min. The column temperature was 30 °C and the UV at 215 nm was used for detection. A standard curve was prepared using muconic acid standard (Sigma-Aldrich).

For triacetic acid lactone (TAL) analysis, an Eclipse Plus C18 column (Agilent Technologies) was used with the same HPLC system. 1% acetic acid in water or acetonitrile was used as the mobile phase at 0.3 mL/min, being ramped from 5% organic to 100% organic over 30 min. The column temperature was 25 °C and the Ultraviolet (UV) at 280 nm was used for detection. A standard curve was prepared using >98.0% purity TAL from TCI America.

For aspartate analysis, an Eclipse Plus C18 column (Agilent Technologies) was used with the same HPLC system. The samples were derivatized with same volume of freshly prepared derivatization agent (0.44 mg/mL o-phthaldialdehyde dissolved in methanol, 100 mM sodium tetraborate—pH 10.5, 0.44 % β-mercaptoethanol). After incubation at room temperature for 1 min, the derivatized product was immediately via HPLC with detection wavelength set to 338 nm. Column oven was held at 25 °C with 1% acetic acid in water or acetonitrile as the mobile phase over the course of the 30-min sequence under the following conditions: 5–10% organic for 10 min, 10–60% organic for 5 min, 60–100% organic for 10 min, 100 to 10% organic for 1.5 min followed by 5% organic for 3.5 min. The constant flow rate was set at 0.4 mL/min. A standard curve was prepared using >99 % purity aspartate from Sigma.

For 5-aminolevulinic acid analysis (5-ALA), Ehrlich assay was used. Specifically, 300 μL of sample was added to 400 μL of acetate buffer (pH = 4.7). 10 μL of ethyl acetoacetate was added and then the solution was

boiled at 100 °C for 15min. After cooling down, 700 μL of freshly prepared Ehrlich's reagent (300 mg p-dimethylaminobenzaldehyde in 15 mL ethanol and 15 mL of concentrated HCl) was added to the solution. After incubating at room temperature for 20min, the absorbance was measured at 556 nm. A standard curve was prepared using 5-ALA from Sigma.

For glucaric acid analysis, *E. coli* strain DH5α with biosensor pJKR-H-CdaR (Addgene 62557) was used. 500 μL of filter-sterilized supernatant was mixed with 500 μL of 2 × LB with 100 mg/L ampicillin and inoculated with *E. coli* biosensors at OD (600 nm) = 0.01. The culture was incubated at 30 °C for 22 h and the fluorescence was measured by flow cytometry. A standard curve was prepared using glucaric acid from Sigma.

2.8. Metabolomic profiling

In preparation for LC-MS analysis, metabolites were extracted from samples using 100% methanol. Briefly, cell-free lysates consisting of 20 μL media, as well as "*in vivo*" samples consisting of cell pellets (50–100 mg) and associated supernatant (1 mL), were frozen and lyophilized dry (FreeZone 2.5 Plus, Labconco). Cell pellets were additionally powderized by bead-beating in a Mini-Beadbeater-96 (BioSpec Products) with a 2 mm stainless steel bead 5 s (2x). To each sample, 500 μL of 100% methanol was added, followed by a brief vortex and sonication in an iced water bath 10 min. Samples were then centrifuged (5000 rpm, 5 min) to pellet debri, supernatant transferred to a 2 mL Eppendorf, then dried in a SpeedVac (SPD111V, Thermo Scientific) and extracts stored at −80 until ready for LC-MS analysis.

In preparation for LC-MS, dried sample extracts were resuspended in 100% MeOH containing isotopically labeled internal standards (5–50 μM of 13C,15N Cell Free Amino Acid Mixture, #767964, Sigma; 1 μg/mL 2-amino-3-bromo-5-methylbenzoic acid, ABMBA, #R435902, Sigma; 10 μg/mL 13C6-trans-trans-muconic acid, #43536, Sigma; 10 μg/mL catechol 13C7, #CLM-1520-1, CIL; 10 μg/mL 13C-trehalose, #TRE-002, Omicron; 10 μg/mL 13C-mannitol, ALD-030, Omicron; 2 μg/mL 13C–15N-uracil, CNLM-3917, CIL; 5.5 μg/mL 15N-inosine, NLM-4264, CIL; 4 μg/mL 15N-adenine, NLM-6924, CIL; 3 μg/mL 15N-hypoxanthine, NLM-8500, CIL; 5 μg/mL 13C–15N-cytosine, #294108, Sigma; 2.5 μg/mL 13C–15N-thymine, CNLM-6945, CIL). Lysate extracts were resuspended in 120 μL and "*in vivo*" pellet and supernatant extracts resuspended in 180 μl, centrifuge-filtered (0.22 μM hydrophilic PVDF membrane, #UFC30GV00, Millipore), then transferred to glass LC-MS vials.

To detect metabolites with LC-MS, chromatography was performed using an Agilent 1290 LC stack coupled to a Q Exactive HF Orbitrap MS (Thermo Scientific, San Jose, CA). Full MS spectra were collected at 60,000 resolution in both positive and negative ionization mode, with MS/MS fragmentation data acquired using stepped then averaged 10, 20 and 40 eV collision energies at 15,000 resolution. Mass spectrometer source settings included a sheath gas flow rate of 55 (au), auxiliary gas flow of 20 (au), sweep gas flow of 2 (au), spray voltage of 3 kV for both positive and negative ionization, and ion transfer tube temperature of 400 °C.

For polar metabolites, mass spectra were collected from m/z range 70-1050, with normal phase chromatography was performed using a HILIC column (InfinityLab Poroshell 120 HILIC-Z, 2.1 × 150 mm, 2.7 μm, Agilent, #683775-924) at a flow rate of 0.45 mL/min with a 2 μL injection volume. Samples were run on the column at 40 °C equilibrated with 100% buffer B (99.8% 95:5 v/v ACN:H2O and 0.2% acetic acid, w/5 mM ammonium acetate) for 1 min, diluting buffer B down to 89% with buffer A (99.8% H2O and 0.2% acetic acid, w/5 mM ammonium acetate and 5 μM methylene-di-phosphonic acid) over 10 min, down to 70% over 4.75 min, down to 20% over 0.5 min, and isocratic elution for 2.25 min, followed by column re-equilibration by returning to 100% B over 0.1 min and isocratic elution for 3.9 min.

For non-polar metabolites, mass spectra were collected from m/z range 80-1200, with reverse phase chromatography performed using a C18 column (Agilent ZORBAX Eclipse Plus C18, Rapid Resolution HD, 2.1 × 50 mm, 1.8 μm) at a flow rate of 0.4 mL/min with a 2 μL injection volume. Samples were run on the C18 column at 60 °C equilibrated with 100% buffer A (100% H2O w/0.1% formic acid) for 1 min, diluting buffer A down to 0% with buffer B (100% methanol w/0.1% formic acid) over 7 min, and isocratic elution for 1.5 min, followed by column re-equilibration by returning to 100% A over 1 min and isocratic elution for 1 min.

Samples consisted of 3-4 biological replicates and 3–4 extraction controls, with sample injection order randomized and an injection blank of 2 μL of 100% MeOH run between each sample, with the blank replaced by an injection of internal standard mix every 3rd sample as well as QC mix every 15 samples.

Untargeted metabolite identification was performed using a Feature-Based Molecular Networking (FBMN) workflow for peak-finding and putative annotation. Here, MZMine 2 (Pluskal et al., 2010) was used to generate a list of features (unique mz coupled with retention time) and filtered to remove isotopes, for which peak height and intensity is calculated for each feature in each sample. Fragmentation spectra for each feature was uploaded to GNPS: Global Natural Products Social Molecular Networking (Wang et al., 2016) a web-based mass spectrometry identification tool, to generate putative compound identifications of each feature based on matching MSMS spectra with one found in the GNPS database (Supplementary Table S6). Raw LC-MS data is available in the MassIVE repository (https://massive.ucsd.edu/) under accession number MSV000092596.

3. Results and discussion

3.1. Portable rewiring in S. cerevisiae and E. coli

We previously demonstrated that the metabolism of a metabolically engineered cell is reflected in cell extracts generated from the respective modified strain (Rasor et al., 2021). This approach increased titers and volumetric productivities of diverse metabolites in cell-free reactions, including 2,3-butanediol, itaconic acid, and glycerol. Here, we sought to create platform strains with enhanced carbon flux toward common nodes of metabolism (Fig. 1) to rapidly diversify cell-free metabolic potential. To do so, we altered the expression level of key genes that regulate carbon flux in central metabolism for both *S. cerevisiae* BY4741 and *E. coli* MG1655 strains using CRISPR/dCas9 systems and plasmid-based expression. Specifically, we conceptualized that a plasmid-based system would be preferrable due to ease of editing and portability across strains.

For *S. cerevisiae*, we employed a dCas9VPR and a single-guide RNA (sgRNA) cassette (Fig. 2A) that is suitable as a dual effector for both repression (CRISPR interference) when being directed into the open reading frame (ORF) and activation when directed to the promoter regions of target genes (Deaner et al., 2018). To acomplish this, a tRNA-gRNA design was applied in the sgRNA cassette (thus enabling expression from a Pol II promoter) and assembled using a one-pot GoldenGate cloning scheme (Zhang et al., 2019). Efficacy was validated in a strain of *S. cerevisiae* that expressed yECitrine (YFP) and mKate2 (RFP) as targets for CRISPRi (Supplementary Fig. S1) and confirmed that dCas9VPR can be used as a multi-target CRISPR interference effector to genomic genes in *S. cerevisiae* (Deaner and Alper 2017).

For *E. coli*, only CRISPR interference was used to achieve multiplexed repression (Fig. 2C) due to the difficulty in identifying PAM sequences within specific promoters (Bikard et al., 2013). Thus, for repression, we built and verified an arabinose-inducible CRISPR system for multiplexed repression in *E. coli* MG1655 using a similar fluorescent marker strain (Supplementary Fig. S2). The strains were grown in LB media with or without 1% glucose and different concentrations of arabinose (%) were added into the media. We found there was no leaky expression of the

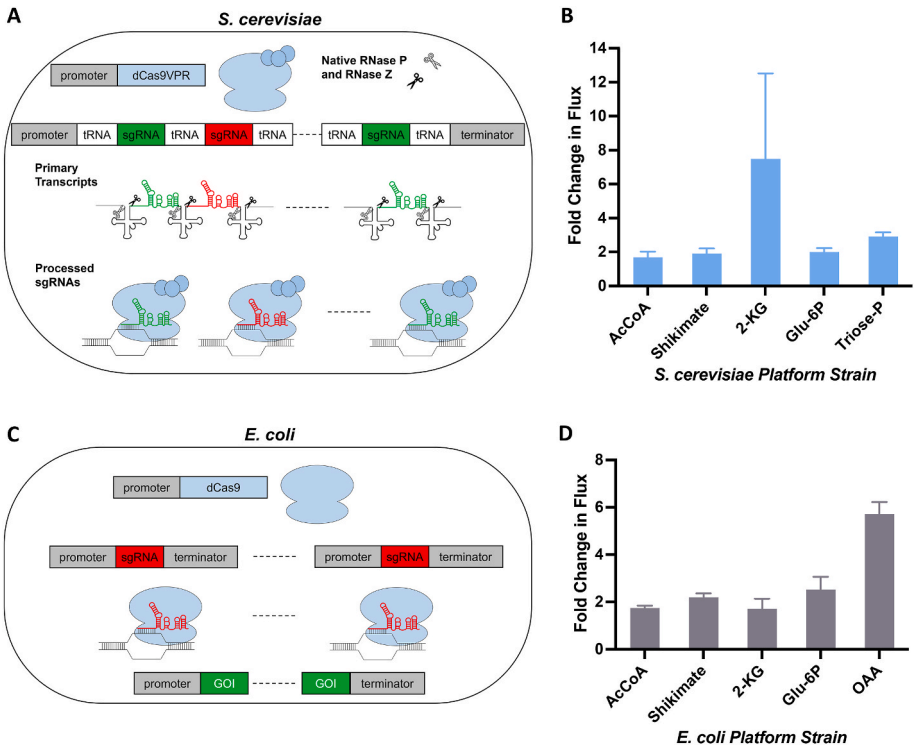

Fig. 2. Multiplexed regulation and validation of platform strains. A) A single dCas9VPR effector was used to regulate gene expressions in S. *cerevisiae* strains for upregulation (green) and repression (red). The sgRNA cassette was assembled using a tRNA-gRNA design and was expressed using Pol II promoter. The primary transcripts were processed into sgRNAs by native RNaseP/Z (Xie et al. 2015). **B)** *S. cerevisiae* platform strains were validated with different strategies. Degree of rewiring was judged by respectively enhanced carbon fluxes compared with control strains (no sgRNA cassette). **C)** To construct the *E. coli* platform strains, selected native genes were over-expressed (green) while dCas9 was used to repress gene expressions (red). The sgRNAs were expressed individually using synthetic promoters. **D)** *E. coli* platform strains were validated with different strategies. Degree of rewiring was judged by respectively enhanced carbon fluxes compared with control strains (no sgRNA cassette and no activation of genes). Data represent mean ± standard deviation of n = 3 technical replicates. Histograms represent *in vivo* data.

rewiring system, and the induction was triggered by low concentration of arabinose regardless of the existence of glucose (Greenblatt and Schleif 1971). For overexpression, we introduced genetically-encoded overexpression of native genes for increased flux.

3.2. Platform strain building and validation

Using this portable rewiring toolbox, we built platform strains in both *S. cerevisiae* BY4741 and *E. coli* MG1655 that are rewired to redirect the carbon flux towards key metabolic nodes *in vivo* (Fig. 1). This metabolic potential will then be "locked-in" during the cell extract preparation and subsequent cell-free metabolism. These key metabolites were selected on their propensity to be precursors for many desirable bioproducts. This led to the selection of strains with enhanced flux toward acetyl-CoA (AcCoA), shikimate, α-ketoglutarate (2-KG), glucose-6-phosphate (Glu-6P), triose-phosphate (Triose-P) and oxaloacetate (OAA). Target genes for overexpression and knockdown/deletion were selected based on both past literature and pathway inspection (Table 1). Both *S. cerevisiae* OAA strain and *E. coli* Triose-P strain were excluded from the list of platform strains as we were not able to validate carbon flux changes in these two strains.

After completing strain construction, we assessed *in vivo* carbon flux by monitoring surrogate, downstream molecules/pathways that required precursors that were the targets of the flux enhancement (Fig. 2). We chose to quantify the improvements based on downstream product yields in *S. cerevisiae* strains (due to varied glucose consumptions across strains) and product titers in *E. coli* strains. For AcCoA platform strains, enhanced carbon flux towards acetyl-CoA was validated by increased heterologous triacetic acid lactone (TAL) production and rewiring led to a nearly 1.7-fold increase in TAL production over the respective control strains for both *S. cerevisiae* and *E. coli* platforms. For shikimate platform strains, the enhanced carbon flux was validated by the increased production of endogenous 3-dehydroshikimate (3-DHS). In this case, metabolic rewiring led to a 1.9-fold increase in 3-DHS production for *S. cerevisiae* and a 2.2-fold increase for *E. coli* compared with control strains. For *S. cerevisiae* Triose-P platform strains, the enhanced carbon flux was validated via endogenous glycerol production in yeast resulting in a 2.9-fold increase over the control strain. The validation of corresponding *E. coli* strains was not feasible as there is no endogenous glycerol production. For 2-KG platform strains, the

Table 1
Gene targets to build platform strains. The platform strains with enhanced carbon flux toward key metabolites shown in Fig. 1 were designed and built with the portable rewiring strategy.

Platform Strains		Acetyl-CoA	Shikimate	α-ketoglutarate	Glucose-6-P	Triose-P	Oxaloacetate
Gene targets in *S. cerevisiae*	Upregulation	*PDC1, ALD6, ACS1*	*TKL1, ARO4*	*PYC1/2, IDH2, IDP1, GDH2*	*PGI1, FBP1*	*GPD1/2*	*Only in E. coli*
	Repression	*CIT2*	*ZWF1*	*GDH1*	*ZWF1*	*TDH3, ADH1/3/5*	
Gene targets in *E. coli*	Over-expression	*aceEF, acs*	*aroG (fbr)*	*ppc, icd*	*pgi, fbp, yagF, glpX*	***Only in S. cerevisiae***	*ppc*
	Repression	*gltA, glcB*	*pykAF*	*gdhA*	*Zwf*		*mdh, aceE*

enhanced carbon flux was validated by increased heterologous 5-aminolevulinic acid (5-ALA) production (Neidle and Kaplan 1993). Metabolic rewiring supported a 7.5-fold and a 1.7-fold increase in 5-ALA production for *S. cerevisiae* and *E. coli* platforms compared with control strains, respectively. For Glu-6P platform strains, the enhanced carbon flux was validated by increased heterologous glucaric acid production (Moon et al., 2009) and resulted in a 2-fold increase in glucaric acid production for *S. cerevisiae* and a 2.4-fold increase for *E. coli* platforms over respective control strains. Finally, for *E. coli* OAA platform strains the enhanced carbon flux was validated by increased aspartate production (Lee et al., 2007) via recombinant expression of a native AspC enzyme and demonstrated a 5.7-fold increase in titer in minimal M9 media compared with the control. However, the validation for *S. cerevisiae* OAA strain was hindered by the existing pool of aspartate in complete synthetic media. Taken together, our rapid rewiring strategy led to a roughly 2-fold increase in the *in vivo* carbon flux towards target metabolites in most of the platform strains (Fig. 2B, D).

3.3. Preparation of platform extracts and cell-free biosynthesis

After validating the results of metabolic rewiring *in vivo*, we generated cell extracts from all 10 platform strains and the 2 wildtype controls for use in cell-free biosynthesis. To test the underlying premise of this work that rewired platform strains will yield more effective cell-free extracts for pathway characterization, we selected two products for more in-depth analysis: triacetic acid lactone as a single-step pathway and muconic acid as a multiple enzyme pathway. For each of these pathway enzymes, 5–10 enzyme variants identified through BLAST searches using literature identified pathways (see Supplementary Table S1 for identity and cut-off thresholds) (Curran et al., 2013; Xie et al., 2006) were synthesized through the JGI DNA Synthesis Science Program. These genes were synthesized with a 5' sequence encoding an N-terminal CAT-strep-linker (the first 5 amino acids of chloramphenicol acetyltransferase, a Strep-tag, and a glycine-serine linker) to improve cell-free expression consistency and facilitate purification after protein synthesis (Kightlinger et al., 2018, 2019). Next, cell-free gene expression was performed by combining cell extract from *E. coli* BL21-Star(DE3) with linear expression templates and the PANOx-SP reaction formulation according to established protocols (Hodgman and Jewett 2013; Jewett et al., 2008; Jewett and Swartz 2004; Kightlinger et al., 2018, 2019; Rasor et al., 2022). Enzymes were purified from cell-free reactions using Strep-Tactin and subsequently dialyzed into a buffer more similar to cell-free reaction compositions. Then cell-free metabolite synthesis was performed by combining extracts with glucose, cofactors, buffer, and the individual or combined purified enzymes.

3.4. Triacetic acid lactone (TAL) pathway screening

TAL is a versatile biochemical that only requires 1 heterologous enzyme (a 2-pyrone synthase (Xie et al., 2006)) to convert central metabolites into TAL (Fig. 3A), enabling a simple and exhaustive comparison of the 10 engineered platform extracts and 2 background strains from both species for their metabolic potential. Combining the purified enzyme with each of these wild-type and platform extracts resulted in a

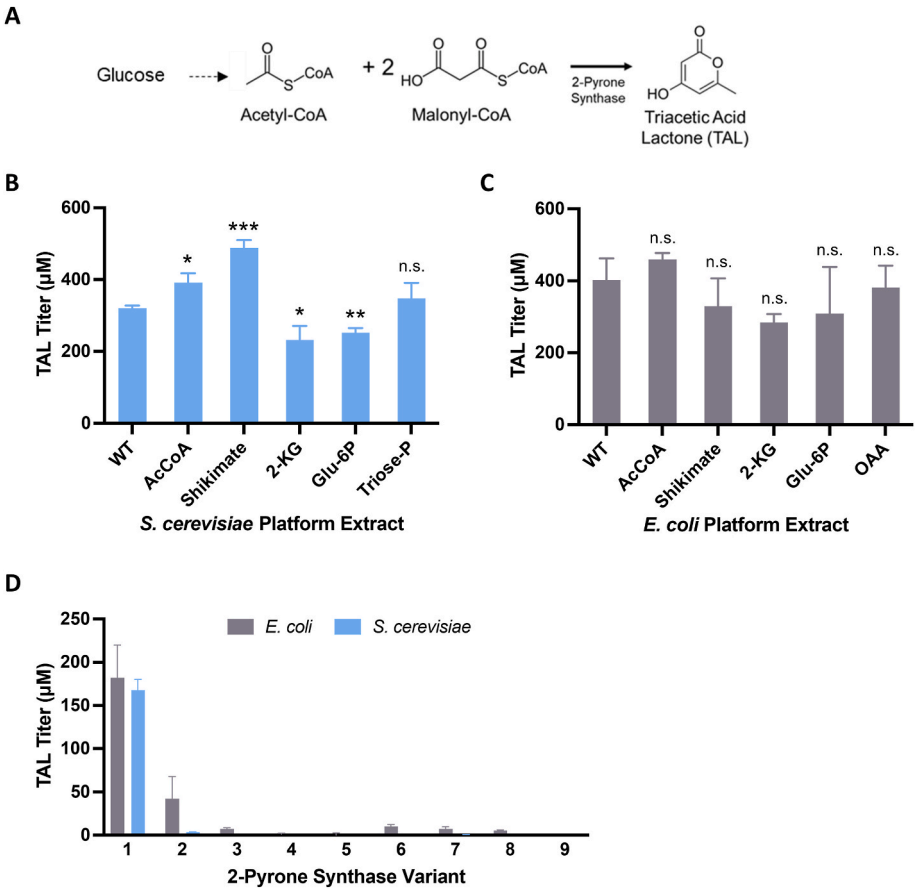

Fig. 3. Cell-free TAL synthesis. A) The biosynthetic pathway for TAL requires endogenous glycolysis and 1 heterologous enzyme. **B–C)** The AcCoA platform extract results in higher TAL titers than wildtype extracts for both *E. coli* and *S. cerevisiae,* respectively, and several other platform extracts also increase TAL synthesis. The statistical significance was calculated based on wild-types using student t-test (n.s.: $p > 0.05$, *: $p \leq 0.05$, **: $p \leq 0.01$, ***: $p \leq 0.001$). **D)** Enzymes identified from literature or BLAST result in lower TAL titers than the canonical 2-pyrone synthase in cell-free reactions with *E. coli* and *S. cerevisiae* extract. Data represent mean ± standard deviation of n = 3 technical replicates. Histograms represent *in vitro* data.

range of TAL production from ~200 to 500 μM depending on the specific extract chosen (Fig. 3B, C). This is the first known example of cell-free metabolic prototyping of the same pathway using extracts from 2 distinct organisms. Consistent with our hypothesis, the *S. cerevisiae* AcCoA platform extracts resulted in higher TAL titers than wildtype extracts (Fig. 3B). Multiple platform extracts produced less TAL than the wildtype as the rewiring was designed for different nodes of metabolism while it was surprising that shikimate platform extracts supported the highest TAL production. We did not observe statistically significant differences in extracts from *E. coli*. We hypothesize that this is due to the centrality of acetyl-CoA in metabolism, meaning that all extracts will maintain relatively high flux through this node. Although the *S. cerevisiae* shikimate platform extracts outperformed the AcCoA extracts by ~25%, our approach still demonstrates increased flux through the desired node of metabolism.

Next, we used the extracts derived from both organisms to test the activity of across a collection of 9 known and putative 2-pyrone synthase mutants (Fig. 3D). In this case, we observed that only one enzyme produced TAL (~35% of the original enzyme only in *E. coli* extracts). The remaining enzymes showed 1–6% activity in both extracts. Despite not identifying an improved enzyme, this experiment, which was carried out in hours, demonstrated the rapid prototyping of putative 2-pyrone synthase enzymes. In addition, the fact that 2-pyrone synthase variant 2 only displayed activities in *E. coli* extracts showcased that cell-free extracts from different organism can provide more information than a singular host.

3.5. *In vivo validation of TAL pathway configurations*

From the results of the *in vitro* testing, it was surprising that multiple platform extracts resulted in greater TAL titers despite rewiring toward different nodes of metabolism. At the onset, it was expected that the AcCoA platform would have provided the highest net pathway flux towards TAL. To test whether these *in vitro* observations could be translated *in vivo*, we introduced the TAL pathway enzyme into all the *S. cerevisiae* and *E. coli* platform strains and measured TAL production (Fig. 4A, C). For *S. cerevisiae*, only the AcCoA platform strains showed increased TAL production. While the TAL production from shikimate platform strains was on par with the control strains, α-ketoglutarate rewiring inhibited TAL production. Similarly, in *E. coli*, the AcCoA platform compared with control strains contributed to the highest TAL titer. However, for these cells, the shikimate platform strains also seemed to support increased TAL production.

The trend of TAL production across different platforms between the *in vivo* and *in vitro* systems (Fig. 4B, D) in this study indicated that cellular rewiring can be maintained and activated in the cell-free extracts. Yet, the correlation was poor as the sample size was small and further research is required to understand how the lack of regulation in cell-free reactions impacts metabolic flux. Next, we sought to validate the prototyping results of 2-pyrone synthase in yeast. All variants tested in cell-free extracts (Supplementary Fig. S3) were introduced into *S. cerevisiae* AcCoA platform strains and the 2-pyrone synthase variant resulted in highest TAL production was predicted from the cell-free prototyping. This suggests that the cell-free platform may be particularly helpful in identifying gene products that have low activity, a feature that we have seen before (Karim et al., 2020).

3.6. *Muconic acid pathway screening*

To assess the impact of flux enhanced platform extracts on a more complex pathway, we next applied our toolkit of engineered strains and extracts for the synthesis of muconic acid from the energy-intensive shikimate pathway. This product requires 3 heterologous enzymes to convert the native 3-DHS intermediate into muconic acid with protocatechuic acid (PCA) and catechol as toxic intermediates (Fig. 5A). We began with a set of enzymes from literature (Pa5 from *Podospora*

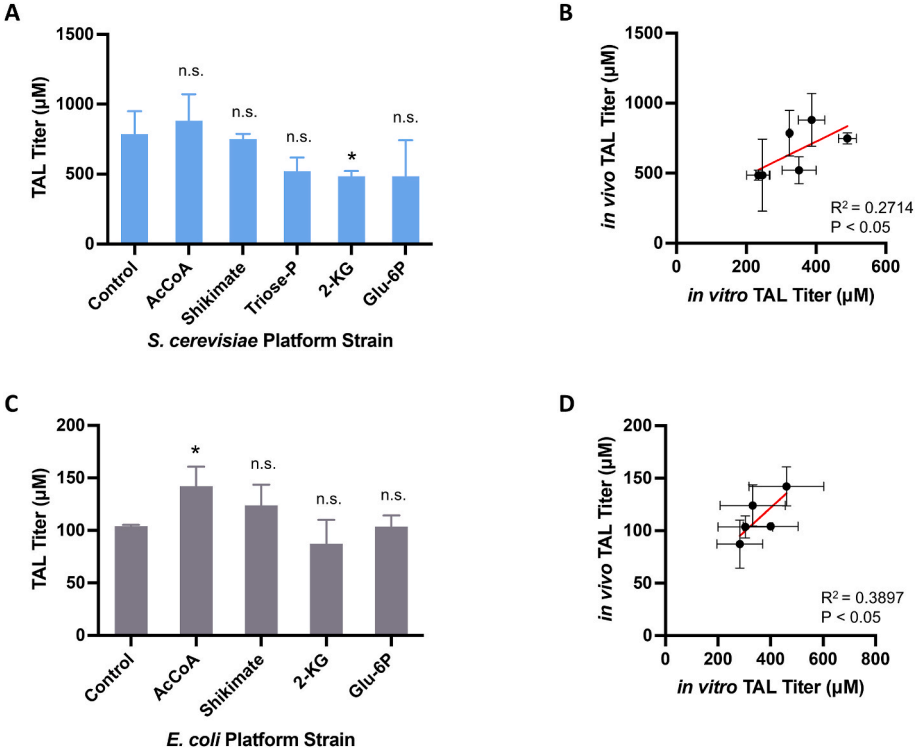

Fig. 4. Cellular TAL synthesis. A, C) TAL production from *S. cerevisiae* and *E. coli* platform strains, respectively. The cloning for OAA-g2ps1-v1 strain was not successful and the fermentation was conducted with only 5 strains. **B)** Correlation of TAL production between *S. cerevisiae in vivo* and *in vitro* platforms. **D)** Correlation of TAL production between *E. coli in vivo* and *in vitro* platforms. The statistical significance was calculated based on controls using student t-test (n.s.: $p > 0.05$, *: $p \leq 0.05$). Data represent mean ± standard deviation of n = 3 biological replicates.

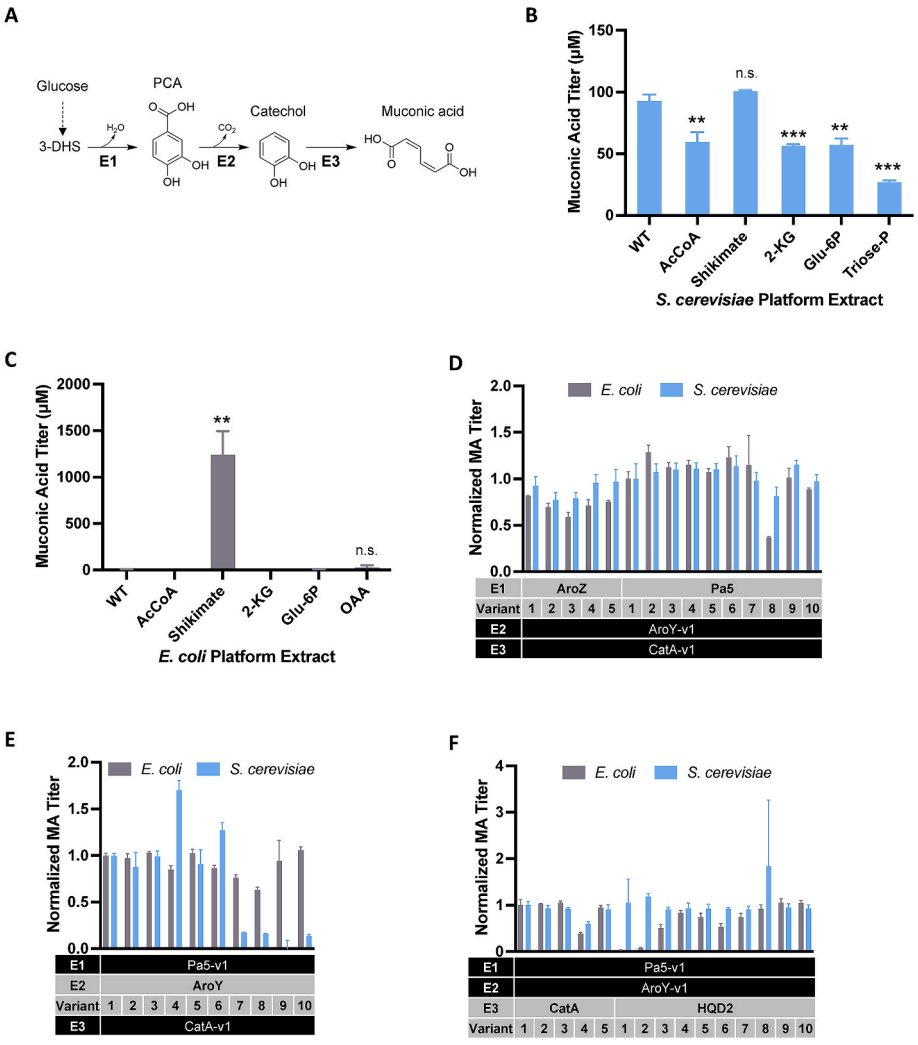

Fig. 5. Applying the engineered toolkit for muconic acid pathway prototyping. A) Muconic acid is produced by 3 heterologous enzymes following glycolysis and the shikimate pathway. **B)** *S. cerevisiae* platform extracts have significantly less flux toward 3-DHS, although engineered 3-DHS platforms still increase product titer over wildtype. **C)** Combining heterologous enzymes with *E. coli* platform extracts shows no muconic acid production without metabolic rewiring for flux toward 3-DHS. The statistical significance was calculated based on wild-types using student t-test (n.s.: $p > 0.05$, *: $p \leq 0.05$, **: $p \leq 0.01$, ***: $p \leq 0.001$). **D)** Cell-free muconic acid titers from a screen of enzyme variants for the conversion of 3-DHS to PCA. **E)** Cell-free muconic acid titers from a screen of enzymes variants for the conversion of PCA to catechol. **F)** Cell-free muconic acid titers from a screen of enzyme variants for the conversion of catechol to muconic acid.

anserina, AroY from *Enterobacter cloacae*, and CatA from *Acinetobacter baylyi* (Curran et al., 2013), the first enzyme variant for each in Supplementary Table S1) and assembled these into the panel of extracts for *S. cerevisiae*, observing sufficient flux through the shikimate pathway to produce muconic acid in all extracts (Fig. 5B). The performance of *S. cerevisiae* extracts was improved by omitting dialysis from the preparation protocol, which retains cellular cofactors and other small molecules (Supplementary Fig. S4). The shikimate platform extract slightly outperformed the wildtype extract and significantly outperformed the other platform extracts. In contrast, the same set of enzymes produced no detectable muconic acid in extract from wildtype *E. coli*, and significant production was only observed in the shikimate platform extracts (Fig. 5C). This highlights the importance of tailoring cells prior to extract preparation as well as differences between the prokaryotic and eukaryotic cell extracts tested here.

We used the *E. coli* shikimate platform extract to combinatorially screen 10 enzyme classes across the 3-step heterologous pathway (Pa5, AroZ from *Klebsiella pneumoniae*, QutC from *Aspergillus nidulans*, or DhsD from *Debaryomyces hansenii* converting 3-DHS to protocatechuic acid (PCA); AroY, FDC from *D. hansenii*, Pa0 from *P. anserina*, and Pa4 from *P. anserina* converting PCA to catechol; CatA and HQD2 from *Candida albicans* converting catechol to muconic acid) and observed activity from a small subset (Pa5, AroZ, AroY, HQD2, and CatA) (Supplementary Fig. S5). This matrix of 32 unique enzyme combinations was built and tested in 3 days, which is significantly faster than screening the same test space *in vivo*.

The enzyme classes with demonstrated activity were investigated further by screening enzyme variants *in vitro* using both *E. coli* and *S. cerevisiae* platform extracts with enhanced 3-DHS flux. We explored 5 variants of AroZ and CatA and 10 variants of Pa5, AroY, and HQD2. Rather than assessing the full combinatorial space (2250 unique combinations), we sequentially changed 1 enzyme from the best-performing combination in our initial comparison of enzyme classes (variant 1 of Pa5, AroY, and CatA) while holding all enzyme concentrations at 0.5 μM. Variants of Pa5 or AroZ were tested with AroY-v1 and CatA-v1; variants of AroY were tested with Pa5-v1 and CatA-v1; and variants of CatA or HQD2 were tested with Pa5-v1 and AroY-v1 to simplify comparisons to the initial set of enzymes. This allowed us to screen all enzyme variants through 45 enzyme combinations built and tested in the context of 2 unique extract backgrounds in only 5 days (Fig. 5D–F). Reactions with *S. cerevisiae* extracts made ~100 μM while those with *E. coli* extracts made ~1200 μM muconic acid, so the results are plotted

as relative titer for ease of comparison on the same plot. Although the trends are qualitatively similar across the 3 steps in both organisms, some enzymes perform much better in one organism's extract. For example, *S. cerevisiae* extracts appear more sensitive to the identity of the second enzyme, which could be a result of differences in cofactor regulation or other background metabolism in the extracts. This cell-free enzyme screening method can identify both more active enzyme variants and highlight metabolic nuances in different strains, providing deeper insights into strain design and pathway enzyme selections.

3.7. *In vivo* validation of muconic acid pathway configurations

Moving forward, we aimed to validate the cell-free prototyping results of muconic acid synthesis using the platform strains engineered for increased flux through the shikimate pathway, which were validated by 3-DHS synthesis up to 2-fold greater than wildtype cells (Fig. 2B, D). The enzyme combinations tested *in vitro* were expressed with the same yeast promoters or the same combination of *E. coli* promoters and ribosome binding sites. These pathways were then introduced into *S. cerevisiae* and *E. coli* shikimate platform strains, respectively, and muconic acid production was measured (Fig. 6A, C; Supplementary Figs. S6A–B). The

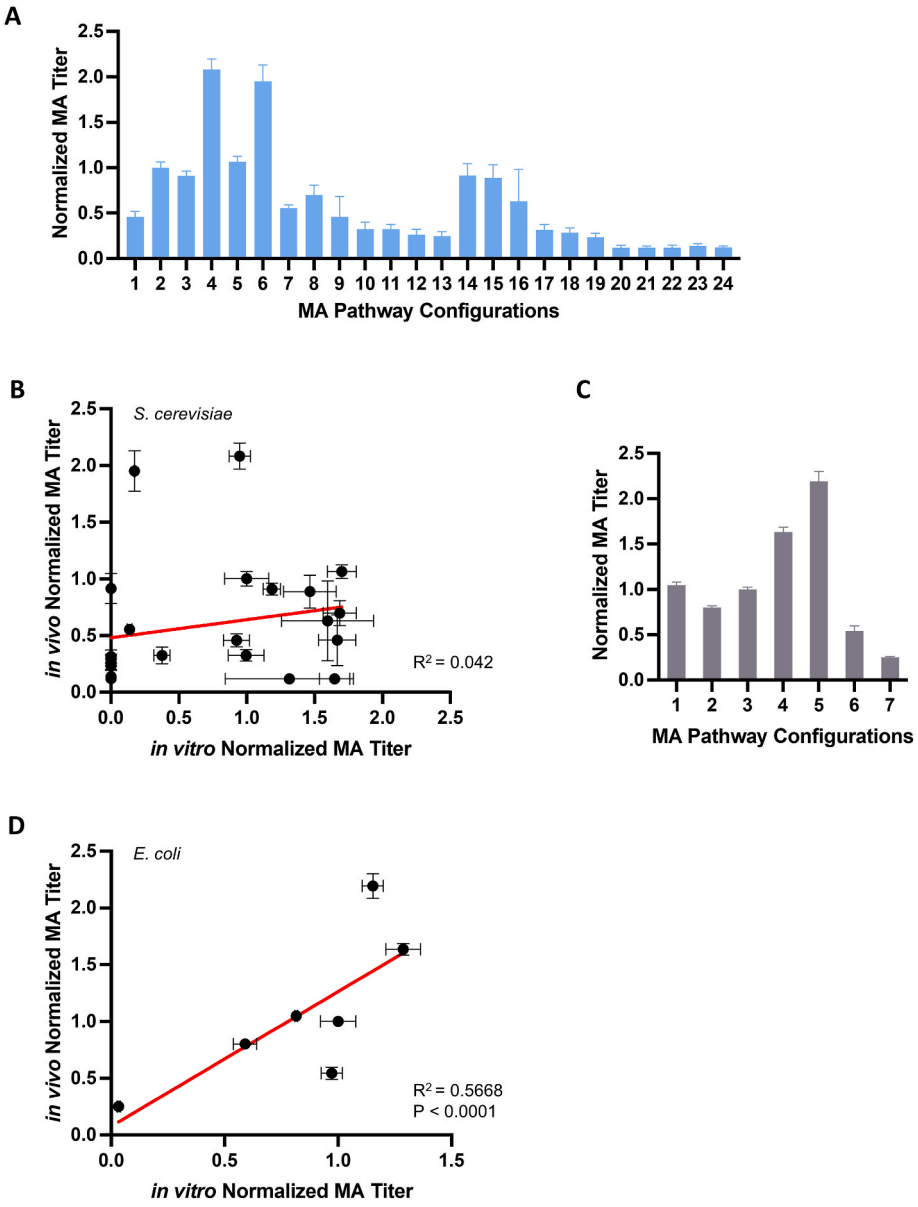

Fig. 6. *In vivo* muconic acid production from different pathway configurations. A) TKL1, ARO4 were activated and ZWF1 were repressed by the CRISPR system in *S. cerevisiae* BY4741 to build shikimate platform strains. **B)** 72 h 3-DHS production in 5% glucose between different rewired strains and control strains. The production was measured as TAL yield per glucose consumed. **C)** The feedback-resistant aroG mutant was overexpressed and *pykA, pykF* were repressed by the CRISPR system to enhance shikimate pathway flux. **D)** 72 h 3-DHS production in M9 media with 2% glucose highlights a 2.3-fold increase in muconic acid titers after metabolic rewiring. **E)** Muconic acid production from *S. cerevisiae* shikimate platform strains with various enzyme combinations (Supplementary Table S4). **F)** Correlation between *S. cerevisiae* fermentations and cell-free reactions was surprisingly low, likely due to complexities in eukaryotic structure or regulation that are not retained *in vitro*. **G)** Muconic acid production from *E. coli* shikimate platform strains with various enzyme combinations (Supplementary Table S4). **H)** Correlation between *E. coli* fermentations and cell-free reactions is relatively high, which enables down-selection of promising pathways prior to strain engineering. Muconic acid titers were normalized to the default configuration (Pa5-v1/AroY-v1/CatA-v1) for each system. Data represent mean ± standard deviation of n = 3 biological replicates.

results displayed marked differences between enzyme variants and these differences were consistent in various combinations. For example, in *S. cerevisiae* strains, Pa5 variant 1 showed better activity compared with variants 2 and 6, with variant 9 being the worst. Yeast strains with HQD2 variants 9 and 10 always produced more muconic acid compared with strains with variants 2 or CatA variant 1, if the other two enzymes were the same (Fig. 6A). Similarly, in *E. coli* strains, HQD2 variants 9 and 10 also led to higher muconic acid titers (Fig. 6C).

Both *in vivo* and *in vitro* muconic acid productions in *S. cerevisiae* (Fig. 6B) and *E. coli* (Fig. 6D) were compared. The muconic acid titer was normalized to the default configuration (Pa5-v1/AroY-v1/CatA-v1), which was 41.2 mg/L and 27.4 mg/L in *S. cerevisiae* and *E. coli* shikimate platform strains, respectively. The best two pathway configurations (AroZ-v4/AroY-v1/HQD2-v9 and AroZ-v4/AroY-v1/HQD2-v10) were also the best performing combinations in the *E. coli* cell-free reactions, in which AroZ variant 4, HQD2 variants 9 and 10 have not been reported in previous works to our knowledge. On the contrary, there is limited correlation between yeast *in vivo* and *in vitro* systems. As studies showed that the best pathway configurations informed by *E. coli* extracts also worked well *in vivo* (Karim et al., 2020), the more complicated regulatory systems and organelle-based compartmentalization in yeast could potentially reduce the transferability from *in vitro* to *in vivo*. Nevertheless, the pathway prototyping in *S. cerevisiae* extracts can contribute to cell-free biomanufacturing where metabolic engineering in cells coupled with *in vitro* reaction optimization can result in elevated titers and productivities compared to traditional fermentations (Grubbe et al., 2020; Rasor et al., 2021).

3.8. Metabolomic comparison between cell-free reactions and in vivo samples

To better characterize the differences between *in vivo* and *in vitro* systems, we used mass spectrometry-based metabolomics to study both cellular and cell-free systems samples for both cell types. The cellular samples were taken from cellular fermentation using either shikimate platform strains or control strains, with or without muconic acid pathway. The cell pellets and supernatants of cellular samples were separated and individually analyzed. The cell-free samples were taken from cell-free reactions using either shikimate platform extracts or control extracts, with or without muconic acid pathway. The samples were run thoroughly with untargeted metabolomics analysis.

A significant number of metabolite features were identified throughout this experiment, but the vast majority did not matched compounds in GNPS (Wang et al., 2016) the metabolomics database. As a result, a principal component analysis (Fig. 7A, Supplementary Fig. S7) was used as a means to classify the various samples based on the unique featured observed in the untargeted analysis. While the differences were larger in cellular samples between *S. cerevisiae* and *E. coli*, the metabolism of cell-free samples were more consistent. This is likely due to the similarity in cell-free reaction composition, with high concentrations of buffer and glutamate salts overshadowing biochemical nuances in the extracts. This separation of cellular and cell-free metabolomics underscores some of the differences seen in the examples above when comparing *in vivo* and *in vitro* results. A more focused analysis on *E. coli* extracts with muconic acid pathway revealed rather substantial differences between shikimate platform extracts and control extracts (Fig. 7B) thus indicating a metabolism change due to the pre-optimization. This result implies that the impact of rewiring was not limited to just a singular metabolite and instead evoked a pleiotropic effect on metabolism. Nevertheless, these results provide a window into the distinct nature of metabolism across these varied samples.

4. Conclusions

The portable rewiring strategy employed here allowed us to develop a toolkit of metabolically rewired bacteria and yeast strains with

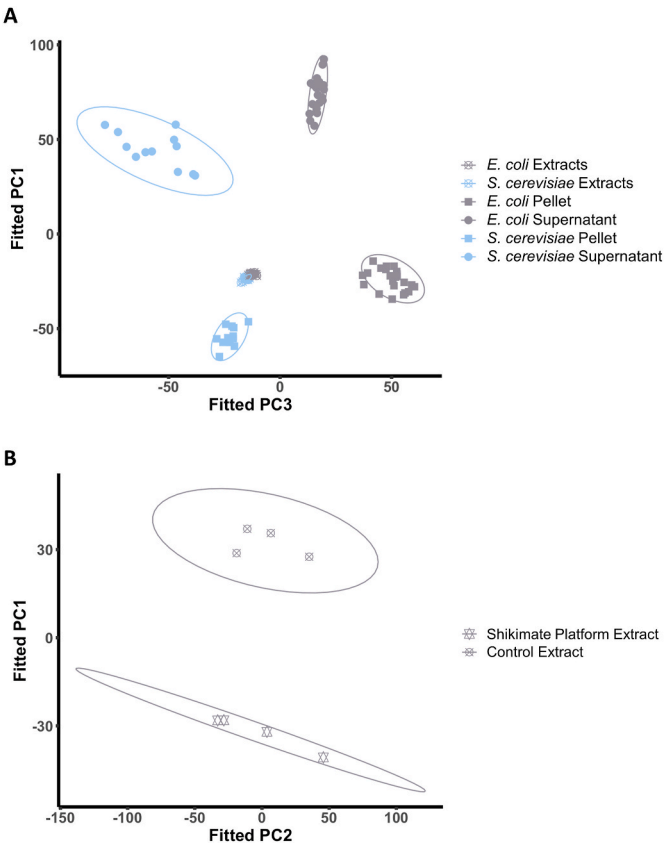

Fig. 7. Metabolomic analysis of cellular and cell-free samples. A) Principal component analysis (PC1 and PC3) on all samples shows tight grouping of cell-free samples in contrast to clear differences in cellular samples. The principal components indicated distinct metabolomic information from cellular and cell-free systems. Within cellular samples, the metabolomic difference between *E. coli* and *S. cerevisiae* was also significant. **B)** Principal component analysis on *E. coli* cell-free samples with muconic acid pathway. The principal components revealed metabolomic change after the extracts were pre-optimized.

increased flux toward common precursors in biochemical production. Corresponding cell extracts prepared from these engineered platform strains enable rapid prototyping of different enzyme combinations and the assessment of uncharacterized enzymes mined from computational tools like BLAST, as demonstrated for TAL and muconic acid production. Both *S. cerevisiae* and *E. coli* cell-free reactions showed moderate correlations to cellular TAL synthesis, but only *E. coli* data aligned *in vivo* and *in vitro* for the more complex synthesis of muconic acid. These pathways also exhibited differences in flux, with cellular rewiring more directly impacting *in vitro* titers for muconic acid than for TAL. We hypothesize that these differences may stem from changes in regulatory mechanisms and compartmentalization in *S. cerevisiae* extracts relative to the source strain, even for the ostensibly simple TAL pathway with one heterologous enzyme. Likewise, it is possible that higher degrees of metabolic rewiring may be necessary to realize flux changes for specific products. Although more fundamental research will be necessary to understand how differences between cells and cell extracts may impact metabolism when complex, multi-organelle processes in eukaryotes are isolated *in vitro*, the engineered toolkit of cells and extracts stands to accelerate the understanding and development of production strains for diverse biochemical products.

Author statement

H.A. and M.J. conceived the project, acquired funding, analyzed results, and wrote the manuscript. X.Y. and B.R. designed experiments,

conducted experiments, analyzed results, and wrote the manuscript. N. B. conducted cell-free experiments. K.L. and T.N. conducted the metabolomics study and analyzed data, wrote portions of the manuscript. A.K. analyzed results, designed experiments, and wrote the manuscript.

Data availability

Data will be made available on request.

Acknowledgements

We thank Nigel Mouncey, Yasuo Yoshikuni, Berkeley Kauffman, Ben Bowen, and Rex Malmstrom from the U.S. Department of Energy Joint Genome Institute for conversations throughout the development of the project. This work was supported by an Emerging Technologies Opportunity Program (ETOP) award under Subcontract No. 7399340 from the U.S. Department of Energy Joint Genome Institute (https://ror.org/04xm1d337), a DOE Office of Science User Facility, is supported by the Office of Science of the U.S. Department of Energy operated under Contract No. DE-AC02-05CH11231. B.J.R. was supported by a National Defense Science and Engineering Graduate Fellowship (Award ND-CEN-017-095). N.B. was supported by a Samuels Family LA-HIP 2.0 Children's Hospital Los Angeles Research Grant.

Appendix A. Supplementary data

Supplementary data to this article can be found online at https://doi.org/10.1016/j.ymben.2023.10.008.

References

Averesch, Nils J.H., Krömer, Jens O., 2018. Metabolic engineering of the shikimate pathway for production of aromatics and derived compounds-present and future strain construction strategies. Front. Bioeng. Biotechnol. 6 (MAR) https://doi.org/10.3389/fbioe.2018.00032.

Bergquist, Peter L., Siddiqui, Sana, Anwar, Sunna, 2020. Cell-free biocatalysis for the production of platform chemicals. Front. Energy Res. 8 https://doi.org/10.3389/fenrg.2020.00193.

Bikard, David, Jiang, Wenyan, Samai, Poulami, Hochschild, Ann, Zhang, Feng, Luciano, A., Marraffini, 2013. Programmable repression and activation of bacterial gene expression using an engineered CRISPR-cas system. Nucleic Acids Res. 41 (15), 7429–7437. https://doi.org/10.1093/nar/gkt520.

Bogart, Jonathan W., Cabezas, Maria D., Vögeli, Bastian, Wong, Derek A., Karim, Ashty S., Jewett, Michael C., 2021. Cell-free exploration of the natural product chemical space. Chembiochem 22 (1), 84–91. https://doi.org/10.1002/cbic.202000452.

Bowie, James U., Sherkhanov, Saken, Korman, Tyler P., Valliere, Meaghan A., Opgenorth, Paul H., Liu, Hongjiang, 2020. Synthetic biochemistry: the bio-inspired cell-free approach to commodity chemical production. Trends Biotechnol. 38 (7), 766–778. https://doi.org/10.1016/j.tibtech.2019.12.024.

Curran, Kathleen A., Leavitt, John M., Karim, Ashty S., Alper, Hal S., 2013. Metabolic engineering of muconic acid production in *Saccharomyces cerevisiae*. Metab. Eng. 15 (1), 55–66. https://doi.org/10.1016/j.ymben.2012.10.003.

Deaner, Matthew, Alper, Hal S., 2017. Systematic testing of enzyme perturbation sensitivities via graded dCas9 modulation in *Saccharomyces cerevisiae*. Metab. Eng. 40, 14–22. https://doi.org/10.1016/j.ymben.2017.01.012.

Deaner, Matthew, Allison, Holzman, Alper, Hal S., 2018. Modular ligation extension of guide RNA operons (LEGO) for multiplexed dCas9 regulation of metabolic pathways in *Saccharomyces cerevisiae*. Biotechnol. J. 13 (9) https://doi.org/10.1002/biot.201700582.

Dudley, Quentin M., Karim, Ashty S., Nash, Connor J., Jewett, Michael C., 2020. *In vitro* prototyping of limonene biosynthesis using cell-free protein synthesis. Metab. Eng. 61, 251–260. https://doi.org/10.1016/j.ymben.2020.05.006.

d'Oelsnitz, Simon, Kim, Wantae, Burkholder, Nathaniel T., Javanmardi, Kamyab, Thyer, Ross, Zhang, Yan, Alper, Hal S., Ellington, Andrew D., 2022. Using fungible biosensors to evolve improved alkaloid biosyntheses. Nat. Chem. Biol. 18 (9), 981–989. https://doi.org/10.1038/s41589-022-01072-w.

Ekas, Holly, Deaner, Matthew, Alper, Hal S., 2019. Recent advancements in fungal-derived fuel and chemical production and commercialization. Curr. Opin. Biotechnol. 57, 1–9. https://doi.org/10.1016/j.copbio.2018.08.014.

Fordjour, Eric, Adipah, Frederick Komla, Zhou, Shenghu, Du, Guocheng, Zhou, Jingwen, 2019. Metabolic Engineering of *Escherichia coli* BL21 (DE3) for *de novo* Production of L-DOPA from D-Glucose. Microb. Cell Factories 18 (1), 1–10. https://doi.org/10.1186/s12934-019-1122-0.

Galanie, Stephanie, Thodey, Kate, Trenchard, Isis J., Filsinger Interrante, Maria, Smolke, Christina D., 2015. Complete biosynthesis of opioids in yeast. Science 349 (6252), 1095–1100. https://doi.org/10.1126/science.aac9373.

Gambacorta, Francesca V., Dietrich, Joshua J., Yan, Qiang, Pfleger, Brian F., 2020. Rewiring yeast metabolism to synthesize products beyond ethanol. Curr. Opin. Chem. Biol. 59, 182–192. https://doi.org/10.1016/j.cbpa.2020.08.005.

Greenblatt, Jack, Schleif, Robert, 1971. Arabinose C protein: regulation of the arabinose operon *in vitro*. Nat. New Biol. 233 (40), 166–170. https://doi.org/10.1038/newbio233166a0.

Grubbe, William S., Rasor, Blake J., Krüger, Antje, Jewett, Michael C., Karim, Ashty S., 2020. Cell-free styrene biosynthesis at high titers. Metab. Eng. 61, 89–95. https://doi.org/10.1016/j.ymben.2020.05.009.

Hodgman, C. Eric, Jewett, Michael C., 2013. Optimized extract preparation methods and reaction conditions for improved yeast cell-free protein synthesis. Biotechnol. Bioeng. 110 (10), 2643–2654. https://doi.org/10.1002/bit.24942.

Jewett, Michael C., Swartz, James R., 2004. Mimicking the *Escherichia coli* cytoplasmic environment activates long-lived and efficient cell-free protein synthesis. Biotechnol. Bioeng. 86 (1), 19–26. https://doi.org/10.1002/bit.20026.

Jewett, Michael C., Calhoun, Kara A., Voloshin, Alexei, Wuu, Jessica J., Swartz, James R., 2008. An integrated cell-free metabolic platform for protein production and synthetic biology. Mol. Syst. Biol. 4 (220) https://doi.org/10.1038/msb.2008.57.

Karim, Ashty S., Jewett, Michael C., 2016. A cell-free framework for rapid biosynthetic pathway prototyping and enzyme discovery. Metab. Eng. 36, 116–126. https://doi.org/10.1016/j.ymben.2016.03.002.

Karim, Ashty S., Jewett, Michael C., 2018. Cell-free synthetic biology for pathway prototyping. Methods Enzymol. 608, 31–57. https://doi.org/10.1016/bs.mie.2018.04.029.

Karim, Ashty S., Dudley, Quentin M., Juminaga, Alex, Yuan, Yongbo, Crowe, Samantha A., Heggestad, Jacob T., Garg, Shivani, Abdalla, Tanus, Grubbe, William S., Rasor, Blake J., Coar, David N., Torculas, Maria, Krein, Michael, Min Eric Liew, Fung, Amy, Quattlebaum, Jensen, Rasmus O., Stuart, Jeffrey A., Simpson, Sean D., Köpke, Michael, Jewett, Michael C., 2020. *In vitro* prototyping and rapid optimization of biosynthetic enzymes for cell design. Nat. Chem. Biol. 16 (8), 912–919. https://doi.org/10.1038/s41589-020-0559-0.

Kelwick, Richard, Ricci, Luca, Mei Chee, Soo, Bell, David, Webb, Alexander J., Freemont, Paul S., 2018. Cell-free prototyping strategies for enhancing the sustainable production of polyhydroxyalkanoates bioplastics. Synthetic Biology 3 (1). https://doi.org/10.1093/synbio/ysy016.

Khatri, Yogan, Hohlman, Robert M., Mendoza, Johnny, Li, Shasha, Lowell, Andrew N., Asahara, Haruichi, Sherman, David H., 2020. Multicomponent microscale biosynthesis of unnatural cyanobacterial indole alkaloids. ACS Synth. Biol. 9 (6), 1349–1360. https://doi.org/10.1021/acssynbio.0c00038.

Kightlinger, Weston, Lin, Liang, Rosztoczy, Madisen, Li, Wenhao, Matthew, P., Milan Mrksich, Delisa, Jewett, Michael C., 2018. Design of glycosylation sites by rapid synthesis and analysis of glycosyltransferases article. Nat. Chem. Biol. 14 (6), 627–635. https://doi.org/10.1038/s41589-018-0051-2.

Kightlinger, Weston, Duncker, Katherine E., Ramesh, Ashvita, Ariel, H., Thames, Aravind Natarajan, Stark, Jessica C., Allen, Yang, Lin, Liang, Mrksich, Milan, DeLisa, Matthew P., Jewett, Michael C., 2019. A cell-free biosynthesis platform for modular construction of protein glycosylation pathways. Nat. Commun. 10 (1) https://doi.org/10.1038/s41467-019-12024-9.

Kwon, Yong Chan, Jewett, Michael C., 2015. High-throughput preparation methods of crude extract for robust cell-free protein synthesis. Sci. Rep. 5 https://doi.org/10.1038/srep08663.

Lee, Kwang Ho, Park, Jin Hwan, Kim, Tae Yong, Kim, Hyun Uk, Lee, Sang Yup, 2007. Systems metabolic engineering of *Escherichia coli* for L-threonine production. Mol. Syst. Biol. 3 (149) https://doi.org/10.1038/msb4100196.

Lee, Michael E., DeLoache, William C., Cervantes, Bernardo, Dueber, John E., 2015. A highly characterized yeast toolkit for modular, multipart assembly. ACS Synth. Biol. 4 (9), 975–986. https://doi.org/10.1021/sb500366v.

Li, Jia-Wei, Zhang, Xiao-Yan, Wu, Hui, Bai, Yun-Peng, 2020. Transcription factor engineering for high-throughput strain evolution and organic acid bioproduction: a review. Front. Bioeng. Biotechnol. 8 https://doi.org/10.3389/fbioe.2020.00098.

Liew, Fungmin Eric, Nogle, Robert, Abdalla, Tanus, Rasor, Blake J., Canter, Christina, Jensen, Rasmus O., Wang, Lan, Strutz, Jonathan, Chirania, Payal, De Tissera, Sashini, Mueller, Alexander P., Ruan, Zhenhua, Gao, Allan, Tran, Loan, Engle, Nancy L., Bromley, Jason C., Daniell, James, Conrado, Robert, Tschaplinski, Timothy J., Giannone, Richard J., Hettich, Robert L., Karim, Ashty S., Simpson, Séan D., Brown, Steven D., Leang, Ching, Jewett, Michael C., Köpke, Michael, 2022. Carbon-negative production of acetone and isopropanol by gas fermentation at industrial pilot scale. Nat. Biotechnol. 40 (3), 335–344. https://doi.org/10.1038/s41587-021-01195-w.

Lim, Hye Jin, Kim, Dong Myung, 2019. Cell-free metabolic engineering: recent developments and future prospects. Methods and Protocols 2 (2), 1–11. https://doi.org/10.3390/mps2020033.

Liu, Yi, Nielsen, Jens, 2019. Recent trends in metabolic engineering of microbial chemical factories. Curr. Opin. Biotechnol. 60, 188–197. https://doi.org/10.1016/j.copbio.2019.05.010.

Liu, Wei, Luo, Zhouqing, Wang, Yun, Pham, Nhan T., Tuck, Laura, Pérez-Pi, Irene, Liu, Longying, Shen, Yue, French, Chris, Auer, Manfred, Marles-Wright, Jon, Dai, Junbiao, Cai, Yizhi, 2018. Rapid pathway prototyping and engineering using *in vitro* and *in vivo* synthetic genome SCRaMbLE-in methods. Nat. Commun. 9 (1), 1936. https://doi.org/10.1038/s41467-018-04254-0.

Milne, N., Thomsen, P., Mølgaard Knudsen, N., Rubaszka, P., Kristensen, M., Borodina, I., 2020. Metabolic Engineering of *Saccharomyces cerevisiae* for the *de novo* Production

of Psilocybin and Related Tryptamine Derivatives. Metab. Eng. 60 (December 2019), 25–36. https://doi.org/10.1016/j.ymben.2019.12.007.

Mingxun, Wang, Carver, Jeremy J., Phelan, Vanessa V., Sanchez, Laura M., Garg, Neha, Peng, Yao, Duy Nguyen, Don, Watrous, Jeramie, Kapono, Clifford A., Luzzatto-Knaan, Tal, Porto, Carla, Bouslimani, Amina, Melnik, Alexey V., Meehan, Michael J., Ting Liu, Wei, Crüsemann, Max, Boudreau, Paul D., Esquenazi, Eduardo, Sandoval-Calderón, Mario, Kersten, Roland D., Pace, Laura A., Quinn, Robert A., Duncan, Katherine R., Chih Hsu, Cheng, Floros, Dimitrios J., Gavilan, Ronnie G., Kleigrewe, Karin, Northen, Trent, Dutton, Rachel J., Parrot, Delphine, Carlson, Erin E., Aigle, Bertrand, Michelsen, Charlotte F., Jelsbak, Lars, Sohlenkamp, Christian, Pevzner, Pavel, Edlund, Anna, McLean, Jeffrey, Piel, Jörn, Murphy, Brian T., Gerwick, Lena, Chuang Liaw, Chih, Liang Yang, Yu, Ulrich Humpf, Hans, Maansson, Maria, Keyzers, Robert A., Sims, Amy C., Johnson, Andrew R., Sidebottom, Ashley M., Sedio, Brian E., Klitgaard, Andreas, Larson, Charles B., Boya, Cristopher A.P., Torres-Mendoza, Daniel, Gonzalez, David J., Silva, Denise B., Marques, Lucas M., Demarque, Daniel P., Pociute, Egle, O'Neill, Ellis C., Briand, Enora, Helfrich, Eric J.N., Granatosky, Eve A., Glukhov, Evgenia, Ryffel, Florian, Houson, Hailey, Mohimani, Hosein, Kharbush, Jenan J., Zeng, Yi, Vorholt, Julia A., Kurita, Kenji L., Charusanti, Pep, McPhail, Kerry L., Fog Nielsen, Kristian, Vuong, Lisa, Elfeki, Maryam, Traxler, Matthew F., Engene, Niclas, Koyama, Nobuhiro, Vining, Oliver B., Baric, Ralph, Silva, Ricardo R., Mascuch, Samantha J., Tomasi, Sophie, Jenkins, Stefan, Macherla, Venkat, Hoffman, Thomas, Agarwal, Vinayak, Williams, Philip G., Dai, Jingqui, Neupane, Ram, Gurr, Joshua, Rodríguez, Andrés M.C., Lamsa, Anne, Zhang, Chen, Dorrestein, Kathleen, Duggan, Brendan M., Almaliti, Jehad, Marie Allard, Pierre, Phapale, Prasad, Felix Nothias, Louis, Alexandrov, Theodore, Litaudon, Marc, Luc Wolfender, Jean, Kyle, Jennifer E., Metz, Thomas O., Peryea, Tyler, Trung Nguyen, Dac, VanLeer, Danielle, Shinn, Paul, Jadhav, Ajit, Müller, Rolf, Waters, Katrina M., Shi, Wenyuan, Liu, Xueting, Zhang, Lixin, Knight, Rob, Jensen, Paul R., Palsson, Bernhard, Pogliano, Kit, Linington, Roger G., Gutiérrez, Marcelino, Lopes, Norberto P., Gerwick, William H., Moore, Bradley S., Dorrestein, Pieter C., Bandeira, Nuno, 2016. Sharing and community curation of mass spectrometry data with global natural products social molecular networking. Nat. Biotechnol. 34 (8), 828–837. https://doi.org/10.1038/nbt.3597.

Moon, Tae Seok, Hwal Yoon, Sang, Lanza, Amanda M., Roy-Mayhew, Joseph D., Kristala, L., Jones, Prather, 2009. Production of glucaric acid from a synthetic pathway in recombinant *Escherichia coli*. Appl. Environ. Microbiol. 75 (3), 589–595. https://doi.org/10.1128/AEM.00973-08.

Moore, Simon J., Lai, Hung-En, Li, Jian, Freemont, Paul S., 2023. Cell-free systems for natural product discovery and engineering. Nat. Prod. Rep. 40 (2), 228–236. https://doi.org/10.1039/D2NP00057A.

Neidle, E.L., Kaplan, S., 1993. Expression of the *Rhodobacter sphaeroides* HemA and HemT genes, encoding two 5-aminolevulinic acid synthase isozymes. J. Bacteriol. 175 (8), 2292–2303. https://doi.org/10.1128/jb.175.8.2292-2303.1993.

O'kane, Patrick T., Dudley, Quentin M., Mcmillan, Aislinn K., Jewett, Michael C., Mrksich, Milan, 2019. High-throughput mapping of CoA metabolites by SAMDI-MS to optimize the cell-free biosynthesis of HMG-CoA. Sci. Adv. 5 (6) https://doi.org/10.1126/sciadv.aaw9180.

Papagianni, Maria, 2012. Recent advances in engineering the central carbon metabolism of industrially important bacteria. Microb. Cell Factories 11, 1–13. https://doi.org/10.1186/1475-2859-11-50.

Pluskal, Tomáš, Castillo, Sandra, Villar-Briones, Alejandro, Orešič, Matej, 2010. MZmine 2: modular framework for processing, visualizing, and analyzing mass spectrometry-based molecular profile data. BMC Bioinf. 11 https://doi.org/10.1186/1471-2105-11-395.

Rasor, Blake J., Yi, Xiunan, Brown, Hunter, Alper, Hal S., Jewett, Michael C., 2021. An integrated *in vivo/in vitro* framework to enhance cell-free biosynthesis with metabolically rewired yeast extracts. Nat. Commun. 12 (1) https://doi.org/10.1038/s41467-021-25233-y.

Rasor, Blake J., Vögeli, Bastian, Jewett, Michael C., Karim, Ashty S., 2022. Cell-free protein synthesis for high-throughput biosynthetic pathway prototyping. Methods Mol. Biol. 199–215. https://doi.org/10.1007/978-1-0716-1998-8_12.

Rogers, Jameson K., Taylor, Noah D., Church, George M., 2016. Biosensor-based engineering of biosynthetic pathways. Curr. Opin. Biotechnol. 42, 84–91. https://doi.org/10.1016/j.copbio.2016.03.005.

Sørensen, Hans Peter, Mortensen, Kim Kusk, 2005. Advanced genetic strategies for recombinant protein expression in *Escherichia coli*. J. Biotechnol. 115 (2), 113–128. https://doi.org/10.1016/j.jbiotec.2004.08.004.

Srinivasan, Prashanth, Smolke, Christina D., 2020. Biosynthesis of medicinal tropane alkaloids in yeast. Nature 585 (7826), 614–619. https://doi.org/10.1038/s41586-020-2650-9.

Tenhaef, Niklas, Stella, Robert, Julia, Frunzke, Noack, Stephan, 2021. Automated rational strain construction based on high-throughput conjugation. ACS Synth. Biol. 10 (3), 589–599. https://doi.org/10.1021/acssynbio.0c00599.

Vögeli, Bastian, Schulz, Luca, Garg, Shivani, Tarasava, Katia, Clomburg, James M., Lee, Seung Hwan, Gonnot, Aislinn, Hakim Moully, Elamar, Kimmel, Blaise R., Tran, Loan, Hunter, Zeleznik, Brown, Steven D., Simpson, Sean D., Mrksich, Milan, Karim, Ashty S., Gonzalez, Ramon, Köpke, Michael, Michael, C., Jewett, 2022. Cell-free prototyping enables implementation of optimized reverse β-oxidation pathways in heterotrophic and autotrophic bacteria. Nat. Commun. 13 (1) https://doi.org/10.1038/s41467-022-30571-6.

Wehrs, Maren, Alexander de Beaumont-Felt, Goranov, Alexi, Harrigan, Patrick, de Kok, Stefan, Lieder, Sarah, Jim Vallandingham, Tyner, Kristina, 2020. You get what you screen for: on the value of fermentation characterization in high-throughput strain improvements in industrial settings. J. Ind. Microbiol. Biotechnol. 47 (11), 913–927. https://doi.org/10.1007/s10295-020-02295-3.

Wu, Gang, Yan, Qiang, Jones, J. Andrew, Tang, Yinjie J., Fong, Stephen S., Koffas, Mattheos A.G., 2016. Metabolic burden: cornerstones in synthetic biology and metabolic engineering applications. Trends Biotechnol. 34 (8), 652–664. https://doi.org/10.1016/j.tibtech.2016.02.010.

Xie, Dongming, Shao, Zengyi, Achkar, Jihane, Zha, Wenjuan, Frost, John W., Zhao, Huimin, 2006. Microbial synthesis of triacetic acid lactone. Biotechnol. Bioeng. 93 (4), 727–736. https://doi.org/10.1002/bit.20759.

Xie, Kabin, Minkenberg, Bastian, Yang, Yinong, 2015. Boosting CRISPR/Cas9 multiplex editing capability with the endogenous tRNA-processing system. Proc. Natl. Acad. Sci. U.S.A. 112 (11), 3570–3575. https://doi.org/10.1073/pnas.1420294112.

Yi, Xiunan, Alper, Hal S., 2022. Considering strain variation and non-type strains for yeast metabolic engineering applications. Life 12 (4), 1–11. https://doi.org/10.3390/life12040510.

Zhang, Yueping, Wang, Juan, Wang, Zibai, Zhang, Yiming, Shi, Shuobo, Nielsen, Jens, Liu, Zihe, 2019. A gRNA-tRNA array for CRISPR-cas9 based rapid multiplexed genome editing in *Saccharomyces cerevisiae*. Nat. Commun. 10 (1), 1–10. https://doi.org/10.1038/s41467-019-09005-3.